# Progress With Applications of Three-Ion ICRF Scenarios for Fusion Research: A Review

Ye.O. Kazakov[1,a)], J. Ongena[1], M. Nocente[2,3], V. Bobkov[4], J. Garcia[5], V.G. Kiptily[6], M. Schneider[7], S. Wukitch[8], J.C. Wright[8], M. Dreval[9,10], K.K. Kirov[6], S. Mazzi[5], R. Ochoukov[4], S.E. Sharapov[6], Ž. Štancar[6], H. Weisen[11], Y. Baranov[6], M. Baruzzo[12], A. Bierwage[13,14], R. Bilato[4], A. Chomiczewska[15], R. Coelho[16], T. Craciunescu[17], K. Crombé[1], E. Delabie[18], E. de la Luna[19], R. Dumont[5], P. Dumortier[1], F. Durodié[1], J. Eriksson[20], M. Fitzgerald[6], J. Galdon-Quiroga[21], D. Gallart[22], M. Garcia-Munoz[21], L. Giacomelli[2], C. Giroud[6], J. Gonzalez-Martin[21], A. Hakola[23], R. Henriques[6,16], P. Jacquet[6], I. Jepu[6,17], T. Johnson[24], A. Kappatou[4], D. Keeling[6], D. King[6], C. Klepper[18], Ph. Lauber[4], M. Lennholm[6], E. Lerche[1], B. Lomanowski[18], C. Lowry[6], M.J. Mantsinen[22,25], M. Maslov[6], S. Menmuir[6], I. Monakhov[6], F. Nabais[16], M.F.F. Nave[16], C. Noble[6], E. Panontin[3], S.D. Pinches[7], A.R. Polevoi[7], D. Rigamonti[3], A. Sahlberg[19], M. Salewski[26], P.A. Schneider[4], H. Sheikh[6], K. Shinohara[27], P. Siren[6], S. Sumida[14], A. Thorman[6], R.A. Tinguely[8], D. Valcarcel[6], D. Van Eester[1], M. Van Schoor[1], J. Varje[11], M. Weiland[4], N. Wendler[15], JET Contributors, the ASDEX Upgrade Team and the EUROfusion MST1 Team

[1] *Laboratory for Plasma Physics, LPP-ERM/KMS, Royal Military Academy, Brussels, Belgium;*
[2] *Dipartimento di Fisica, Università di Milano-Bicocca, Milan, Italy;*
[3] *Institute for Plasma Science and Technology, National Research Council, Milan, Italy;*
[4] *Max-Planck-Institut für Plasmaphysik, Garching, Germany;*
[5] *CEA, IRFM, Saint-Paul-Lez-Durance, France;*
[6] *United Kingdom Atomic Energy Authority (UKAEA), Culham Centre for Fusion Energy (CCFE), Culham Science Centre, Abingdon, UK;*
[7] *ITER Organization, Route de Vinon-sur-Verdon, 13067 St. Paul-lez-Durance, France;*
[8] *Plasma Science and Fusion Center, MIT, Cambridge MA, USA;*
[9] *V.N. Karazin Kharkiv National University, Kharkiv, Ukraine;*
[10] *NSC 'Kharkiv Institute of Physics and Technology', Kharkiv, Ukraine;*
[11] *Tokamak Energy Ltd, Milton Park, United Kingdom;*
[12] *ENEA for EUROfusion, Frascati (Roma), Italy;*
[13] *QST Rokkasho Fusion Institute, Rokkasho, Japan;*
[14] *QST Naka Fusion Institute, Ibaraki, Japan;*
[15] *Institute of Plasma Physics and Laser Microfusion (IPPLM), Warsaw, Poland;*
[16] *Instituto de Plasmas e Fusão Nuclear, IST, Lisbon, Portugal;*
[17] *National Institute for Laser, Plasma and Radiation Physics (NILPRP), Bucharest, Romania;*
[18] *Oak Ridge National Laboratory, Oak Ridge, Tennessee, USA;*
[19] *Laboratorio Nacional de Fusión, CIEMAT, Madrid, Spain;*
[20] *Uppsala University, Uppsala, Sweden;*
[21] *University of Seville, Seville, Spain;*
[22] *Barcelona Supercomputing Center (BSC), Barcelona, Spain;*
[23] *VTT Technical Research Centre of Finland, Espoo, Finland;*
[24] *KTH Royal Institute of Technology, Stockholm, Sweden;*
[25] *ICREA, Barcelona, Spain;*
[26] *Dept. of Physics, Technical University of Denmark, Kgs. Lyngby, Denmark;*
[27] *The University of Tokyo, Kashiwa, Japan;*

[a)] Corresponding author: yevgen.kazakov@rma.ac.be

**Abstract.** The viability of magnetic confinement fusion as an energy source depends on achieving the high ion temperatures required for D-T fusion. Among the available techniques, plasma heating with waves in the ion cyclotron range of frequencies (ICRF) is a prominent method for bulk ion heating in fusion plasmas. Furthermore, a detailed understanding of the non-linear physics of alpha heating and the complex impact of MeV-range fast ions on plasma dynamics becomes progressively more important. This paper provides a comprehensive overview of recent developments with the three-ion ICRF scenarios on Alcator C-Mod, ASDEX Upgrade and JET tokamaks. The results demonstrate the flexibility of these novel scenarios for heating bulk ions in D-T ≈ 50%-50% plasmas and efficient generation of MeV-range fast ions in multi-ion species plasmas. Several key results relevant for ITER and future fusion reactors are highlighted.

## INTRODUCTION

Auxiliary plasma heating is crucial for achieving high ion temperatures necessary for D-T fusion in future magnetic confinement fusion reactors. One flexible technique for plasma heating is the use of waves in the ion cyclotron range of frequencies (ICRF), which has several efficient heating scenarios [1–4]. Among these, the minority heating scenarios [5] are particularly useful in toroidal magnetic fusion research as they feature strong damping of RF waves propagating in the plasma. In minority heating scenarios, electromagnetic waves are absorbed by a small number of resonant ions that have a different cyclotron frequency than that of the main plasma ions. These RF-heated minority ions then transfer their energy through Coulomb collisions to other plasma particles such as bulk ions and electrons. The amount of bulk ion and electron heating depends on the ratio of the fast-ion energy to the critical energy $E_{\mathrm{crit}}$ defined as $E_{\mathrm{crit}} = 14.8 A_{\mathrm{fast}} T_e (\sum_i X_i Z_i^2/A_i)^{2/3}$ [6]. Here, $A_{\mathrm{fast}}$ is the atomic mass of the energetic ions, $T_e$ is the electron temperature, while the concentration, the charge state, and the atomic mass of the thermal ion species are represented by $X_i = n_i/n_e$, $Z_i$, and $A_i$, respectively.

In magnetic fusion devices, fast ions with MeV-range energies primarily heat the plasma electrons. However, it is possible to achieve dominant heating of bulk ions by selecting resonant ions with higher atomic masses as RF absorbing ions and tailoring the fast-ion energies within the range of $E_{\mathrm{crit}}$ or below.

In recent years, there has been a growing interest in exploring new methods for heating fusion plasmas using radiofrequency (RF) waves. Three-ion ICRF scenarios [7–10] is a promising approach that showed its high efficiency for heating plasma mixtures that contain hydrogen and helium isotopes like D-T, H-D, H-$^4$He, and D-$^3$He. These ICRF scenarios require plasma composition to extend beyond two thermal ion species and to include an additional, third ion population. The resonant wave-particle interaction condition $\omega = \omega_{\mathrm{ci}} + k_{\|} v_{\|}$ (here, $\omega = 2\pi f$, $f$ is the frequency of the launched RF waves; $\omega_{\mathrm{ci}}$ is the local cyclotron frequency of resonant ions; $k_{\|}$ and $v_{\|}$ are the wavenumber and ion velocity parallel to the confining magnetic field) is satisfied near one of the ion-ion hybrid (IIH) layers in these multi-ion species plasmas [11, 12]. This is the region where the left-hand polarized RF electric field component, rotating in the direction of the plasma ions and facilitating damping of ICRF waves by the ions, is greatly amplified [13, 14]. By selecting the right plasma composition to satisfy these conditions, ICRF power absorption can be optimized in fusion devices. Furthermore, this method can also be enhanced by using intrinsic and extrinsic impurities like $^9$Be, Ne, and Ar. This allows for further optimization of RF plasma heating in various plasma mixtures.

Throughout the paper, we will use the $Y_2$-($Y_3$)-$Y_1$ notation to refer to the three-ion ICRF scenarios. The indices '1' and '2' denote the non-resonant ion species $Y_1$ and $Y_2$, respectively, ordered according to their $Z/A$ value (i.e., we choose $\omega_{c2} < \omega_{c1}$). Index '3' is reserved for the resonant ions $Y_3$, which are encapsulated in round brackets. It is important to note that there are two equivalent options available for the choice of the resonant absorbers. The original theoretical formulation of these ICRF scenarios, as proposed in Ref. [7], involved a population of ions with a charge-to-mass ratio 'sandwiched' between the two non-resonant ions, i.e. $(Z/A)_2 < (Z/A)_3 < (Z/A)_1$. In this case, ion cyclotron absorption by resonant ions at extremely low concentrations ($X_3 < 1\%$) can be maximized in multi-ion plasmas with plasma composition $X_1 \gtrsim X_1^*$ and $X_2 \lesssim X_2^*$, where

$$X_1^* = \frac{1}{Z_1}\frac{(Z/A)_1 - (Z/A)_3}{(Z/A)_1 - (Z/A)_2}, X_2^* = \frac{1}{Z_2}\frac{(Z/A)_3 - (Z/A)_2}{(Z/A)_1 - (Z/A)_2}\,. \quad (1)$$

Maximizing the absorbed RF power per resonant ion strongly enhances the efficiency of fast-ion generation with ICRF, as shown by Figure 1, which illustrates that nearly all RF power can be channeled to $^3$He ions at concentrations as low as $n(^3\mathrm{He})/n_e \approx 0.1$-$0.2\%$ in mixed H-D ≈ 70%-30% plasmas at JET.

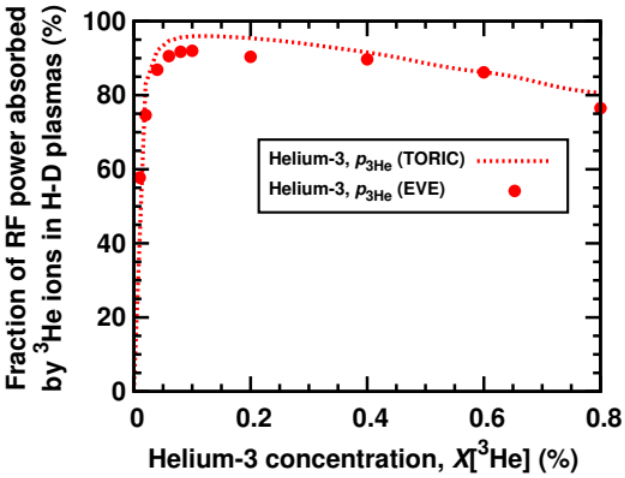


**FIGURE 1.** Three-ion ICRF scenarios and their high potential for generating fast ions in fusion plasmas were identified in Ref. [7]. The figure shows one of the main results predicted by theory: efficient absorption of RF power by a very small number of $^3$He ions (e.g., at $n(^3\text{He})/n_e \approx 0.1$-$0.2\%$) in mixed H-D ≈ 70%-30% plasmas. Reprinted with stylistic modifications from Ye.O. Kazakov et al., *Nucl. Fusion* **55**, 032001 (2015). Reproduced courtesy of IAEA. Copyright 2015 EURATOM.

Fast ions with the same charge-to-mass ratio as one of the main plasma ions can also be used as resonant absorbers. To make the heating scenario work, the third ion population should have sufficiently large parallel velocities such that they can resonate at the IIH layer because of their large Doppler shift. Fast ions injected by neutral beam injection (NBI) are a natural choice for the realization of the Doppler-shifted version of the three-ion ICRF scenario. This technique allows for the exploration of new synergies between ICRF and NBI heating systems, and can accelerate fast ions from their starting energies on the order of 100 keV to MeV-range energies. The application of this synergetic ICRF-NBI scenario at JET leads to a very efficient generation of passing fast ions, and thus the resulting fast-ion distribution mimics closely the distributions generated by negative-NBI systems in the future tokamaks JT-60SA and ITER. For the plasma composition required to realize this ICRF scenario, refer to Eqs. (6) and (7) in Ref. [10].

## EU-US COLLABORATION: PROOF-OF-PRINCIPLE EXPERIMENTS ON ALCATOR C-MOD, JET AND ASDEX UPGRADE TOKAMAKS

In April 2015, theoretical and modeling predictions suggesting the high efficiency of these novel ICRF scenarios were presented at the 21st RF Topical Conference in Lake Arrowhead, USA [15]. A collaborative effort between EU and US researchers was established thereafter to experimentally verify the potential of these novel scenarios on existing tokamaks. A series of proof-of-principle ICRF studies was conducted on the tokamaks Alcator C-Mod (MIT-PSFC, USA) and JET (Culham, UK) during 2015-2016, and first results from both devices validated theoretical predictions. The experiments demonstrated the high efficiency of the three-ion D-($^3$He)-H ICRF scenario for heating mixed H-D plasmas with a small amount of $^3$He ions, see Fig. 2. The optimal $^3$He concentration for the Alcator C-Mod experiments was shown to be approximately $n(^3\text{He})/n_e \approx 0.5\%$, while lower $^3$He concentrations of ~0.2% were successfully applied for heating JET plasmas.

Both tokamak experiments also confirmed the high efficiency of the novel ICRF scenarios for generating energetic ions in the plasma. In the case of JET plasmas, the efficiency of fast $^3$He generation was enhanced by utilizing the asymmetric co-current ICRF antenna phasing ($+\pi/2$ phasing) and taking advantage of the RF-induced pinch effect [16, 17]. The strong core localization of fast $^3$He ions in JET plasmas was also independently confirmed by gamma-ray measurements. The right panel of Fig. 2(b) shows the reconstructed high-energy gamma-ray emission in JET pulse #90753 (3.2T/2.0MA, $f \approx 33$ MHz). It is important to note that most of the energetic $^3$He ions are concentrated in the plasma core and have passing (stagnation) orbits [18]. The main findings of the proof-of-principle experiments with the three-ion D-($^3$He)-H ICRF scenario conducted at Alcator C-Mod and JET tokamaks were summarized in the October 2017 issue of the journal Nature Physics [8].

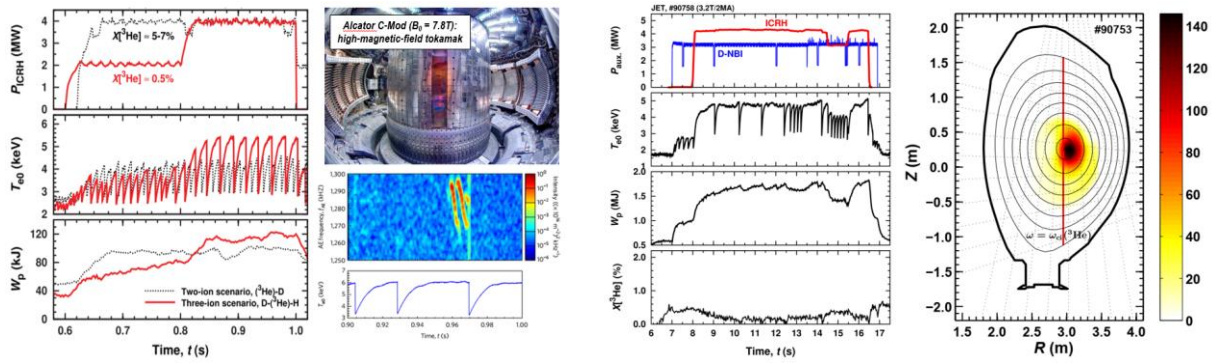


(a) (b)

**FIGURE 2.** Proof-of-principle experiments on Alcator C-Mod (a) and JET (b) tokamaks have successfully demonstrated the high efficiency of three-ion ICRF scenarios for plasma heating and generation of energetic ions. The right panel of Fig. 2(a) shows the sawtooth stabilization and the observation of fast-ion-driven Alfvén eigenmodes in Alcator C-Mod experiments. The right panel of Fig. 2(b) shows the JET plasma poloidal cross-section, together with the reconstructed high-energy gamma-ray emission, illustrating the population of the confined energetic $^3$He ions with $E(^3\text{He}) > 1\text{-}2$ MeV. Note that most of energetic $^3$He ions are strongly localized in the plasma core and have passing (stagnation) orbits [18]. Reprinted with stylistic modifications with permission of Springer Nature from Ye.O. Kazakov et al., *Nature Physics* **13**, 973 (2017). Copyright 2017 EURATOM.

In July 2016, JET successfully demonstrated the Doppler-shifted three-ion ICRF scenario with fast D-NBI ions ($E_{\text{NBI}} \approx 100$ keV) as resonant absorbers for heating mixed H-D plasmas. The results of this scenario were presented at the 22nd RF Topical Conference in Aix-en-Provence, France (June 2017) [9] and later detailed in a paper [19]. The fast-ion observations were successfully reproduced by TRANSP-TORIC and PION modeling [20, 21]. The tomographic reconstruction of the neutron emission showed that the MeV-range D ions generated with the three-ion D-($D_{\text{NBI}}$)-H scenario were strongly core localized (see also [22]), with the same orbit topology as resonant $^3$He ions in the D-($^3$He)-H ICRF experiments. The important consequences of this rather special topology for the resonant fast ions will be discussed in the next sections of this paper.

In 2018, the four leading authors of Ref. [8] received the 2018 APS-EPS Landau-Spitzer Award for the experimental verification of these novel and highly efficient ICRF scenarios on EU and US tokamaks.

In July 2017, the three-ion D-($^3$He)-H ICRF scenario was also demonstrated on the tokamak ASDEX Upgrade (Garching, Germany) [10, 23]. Guided by the ITER needs, significant progress with the development of these ICRF scenarios has been achieved on JET and AUG, as detailed in the Physics of Plasmas review paper [10]. Further progress has been achieved since then, including the application of these ICRF scenarios in non-active and D-T plasmas, relevant for ITER. The key observations from these new experiments are summarized in the following sections.

## FAST IONS AS A TOOL FOR PLASMA CONTROL AND ENHANCED PERFORMANCE AT JET

Alpha particles with energies in the megaelectron volt (MeV) range are expected to be the primary source of plasma heating in future fusion reactors. However, instead of heating fuel ions, the energy of these alpha particles is mainly transferred to the electrons in the plasma. The temperature of the fuel D and T ions will be largely determined by the combined effect of the transfer of power from electrons to bulk ions, as well as the ion-temperature-gradient (ITG) instability. A recent study predicts a beneficial impact of alpha particles on the ITG instability in high-beta ITER plasmas [24].

The presence of MeV-range alpha particles in fusion plasmas is also expected to generate a range of fast-ion phenomena, such as the stabilization of sawtooth oscillations, possible destabilization of different types of fast-ion-driven Alfvén eigenmodes (AEs), and modification of the plasma equilibrium. In present-day fusion experiments, the fraction of MeV-range fast ions in the plasma core is low, allowing for the study of fast-ion effects individually [25]. However, in future burning plasmas, a non-linear coupling between different fast-ion effects is expected, including the impact of fast ions on the ITG instability. Therefore, experimental studies accompanied by modeling of plasmas with a large population of MeV-range fast ions are needed in present-day devices to better understand the extrapolation of alpha heating in future plasmas.

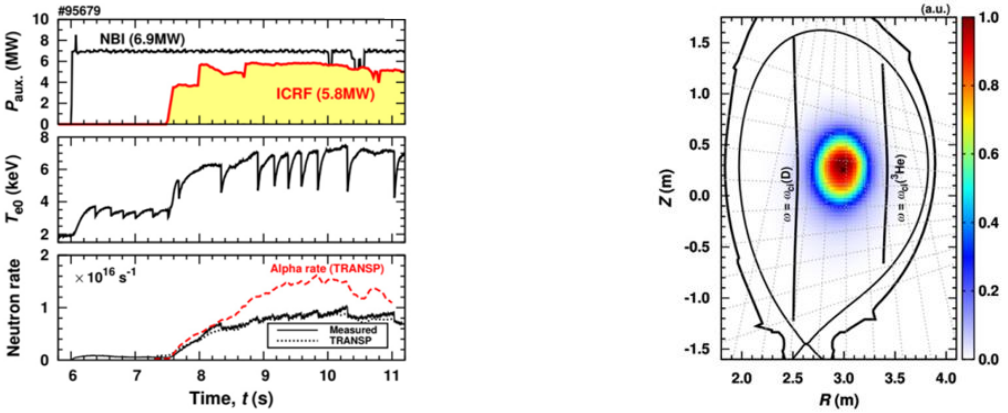


(a) (b)

**FIGURE 3.** JET studies with the three-ion D-($D_{NBI}$)-$^3$He scenario in D-$^3$He plasmas revealed a range of new synergistic fast-ion phenomena, relevant for ITER and future burning plasmas. (a) Overview of JET pulse #95679 (3.7T/2.5MA, $n_{e0} \approx 6\times10^{19}$ m$^{-3}$, $n(^3He)/n_e \approx$ 20-25%). Note the strong increase in the neutron and alpha-particle generation rates during the combined ICRF + NBI heating phase. (b) The measured spatial profile of the D-D neutron emission, clearly illustrating the generation of high-energy D ions in the plasma core with this novel ICRF scheme. Figure 3(a) reprinted from J. Mailloux et al., *Nucl. Fusion* **62**, 042026 (2022), with the original data source from M. Nocente et al., *Nucl. Fusion* **60**, 124006 (2020). Figure 3(b) reprinted from M. Nocente et al., *Nucl. Fusion* **60**, 124006 (2020). Reproduced courtesy of IAEA. Copyright EURATOM.

To gain a deeper understanding of such plasmas, a series of dedicated experiments in D-$^3$He plasmas was conducted at JET using the three ion D-($D_{NBI}$)-$^3$He ICRF scenario [10, 26]. This scenario allows for the acceleration of NBI deuterons with injection energies of ~100 keV to higher energies using ICRF waves. The developed experimental scenario provides unique conditions on JET to probe several aspects of future burning plasmas without introducing tritium. Figure 3(a) shows an overview of JET pulse #95679 (3.7T/2.5MA, $n(^3He)/n_e \approx$ 20-25%, $f \approx$ 33 MHz, dipole phasing), where ~6 MW of ICRF was applied in combination with ~7 MW of NBI. The efficient generation of MeV-range deuterium ions with ICRF in the plasma core (see Fig. 3(b)) resulted in the increase of the D-D neutron rate from ~$0.6\times10^{15}$ s$^{-1}$ in the NBI-only phase to ~$1.0\times10^{16}$ s$^{-1}$ in the combined ICRF + NBI phase of the pulse. These JET plasmas also included a significant population of core-localized alpha particles originating from D-$^3$He fusion reactions: D + $^3$He → $^4$He (3.6 MeV) + $p$ (14.7 MeV) [27]. As follows from Fig. 3(a), the production rate of alpha particles in these plasmas, $R_\alpha \approx$ 1-2$\times10^{16}$ s$^{-1}$ exceeded the D-D neutron rate [28].

Surprisingly, JET experiments showed that the ion temperature efficiently increased in these plasmas with fast-ion electron heating and Alfvénic instabilities, resulting in $T_i \approx T_e$. Additional transport analysis featured that the ITG turbulence was almost entirely suppressed in these plasmas in the presence of a high number of MeV-range fast ions in the plasma core and fully developed Alfvénic activities [29, 30]. This nonlinear mechanism holds promise for a more economical operation of ITER and future fusion reactors that rely on alpha particle heating.

Figure 4(a) depicts the typical distribution function of ICRF-accelerated D ions, as calculated by the TRANSP-TORIC code (see [31, 32]). In turn, Fig. 4(b) shows the computed distribution of the left-hand polarized RF electric field $|E_+|^2$, together with the characteristic orbit of resonant D ions ($E_D$ = 0.8 MeV, $\lambda = v_{||}/v$ = 0.4, white line). These figures illustrate the unique ability of this ICRF scenario at JET to generate a significant number of high-energy ions with passing (stagnation) orbits ($E_D \approx$ 1 MeV, $\lambda \approx$ 0.3-0.5). Notably, the three-ion ICRF scheme produces a fast-ion population with comparable characteristics as high-energy neutral beam injection (N-NBI) systems at JT-60U, JT-60SA and ITER, allowing for the study of various aspects of the interaction of super-Alfvénic passing fast ions also at JET. A detailed discussion on the effectiveness of three-ion ICRF scenarios for producing passing fast ions and fast-ion current drive is provided in Section III-B of Ref. [10]. In summary, the energy-dependence of the pitch parameter of the resonant ions is given by

$$\lambda(E) = \sqrt{\lambda_0^2 \frac{E_0}{E} + \lambda_\infty^2 \left(1 - \frac{E_0}{E}\right)}, \tag{2}$$

where $\lambda_0$ and $E_0$ are the initial pitch and energy of resonant ions, $\Lambda_\infty = \omega_{cD}(0)/\omega \approx$ 0.85-0.89, and $\lambda_\infty = (1 - \Lambda_\infty)^{1/2}$. In case of tangential NBI injectors at JET, resonant D ions are characterized by $E_0 \approx$ 100 keV and $\lambda_0 \approx$ 0.62. Accordingly, at high energies the pitch parameter of the ICRF-accelerated deuterons reaches $\lambda_\infty \approx$ 0.34-0.38, consistent with TRANSP-TORIC modeling results [31, 32].

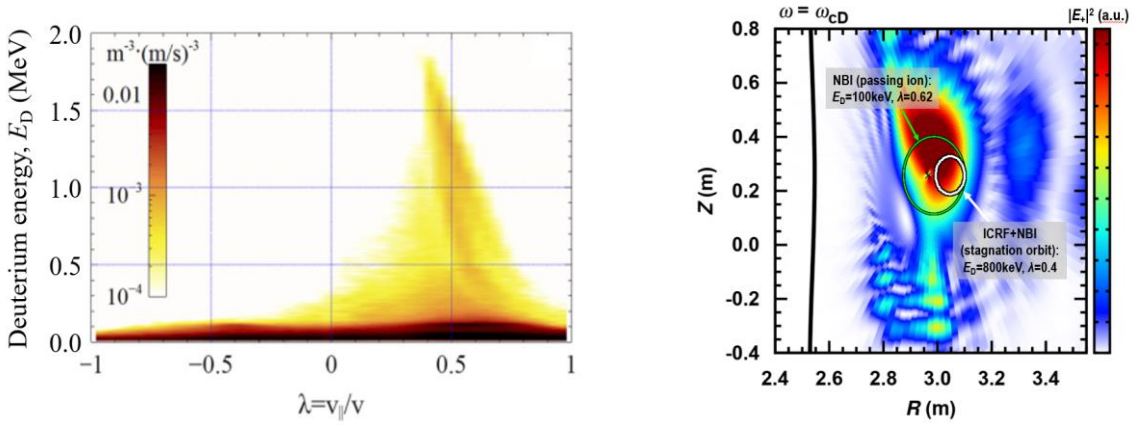


(a) (b)

**FIGURE 4.** Three-ion ICRF scenarios are efficient in generating a large amount of passing fast ions ($v_{\parallel} > 0$) at JET. (a) A typical distribution function of the energetic D ions generated with the D-($D_{NBI}$)-$^3$He scenario, as computed by the TRANSP-TORIC code. (b) A characteristic orbit of resonant D ions ($E_D$ = 0.8 MeV, $\lambda$ = 0.4, white curve), together with the computed distribution of the left-hand polarized RF electric field $|E_+|^2$, as evaluated by TORIC. The figure also shows the computed orbit of the passing NBI fast ions with $E_D$ = 0.1 MeV and $\lambda$ = 0.62 (green curve). Figure 4(a) reprinted with permission from M. Dreval et al., *Nucl. Fusion* **62**, 056001 (2022). Reproduced courtesy of IAEA. Copyright 2022 EURATOM.

In JET D-$^3$He plasmas heated with the three-ion ICRF scenario, a wide range of Alfvén eigenmodes were destabilized by fast ions [32–36]. These include Toroidicity-Induced AEs (TAEs), Ellipticity-Induced AEs (EAEs), and Reversed-Shear AEs (RSAEs), see Fig. 5(a). RSAEs originate from the presence of a local minimum in the safety factor $q_{min}$. Remarkably, two distinct types of centrally localized RSAEs were consistently observed during the long-period sawtooth phases in this series of JET experiments [32]. Notably, in addition to the low-frequency RSAEs with frequencies below the TAE frequency ($f \approx$ 80-180 kHz), high-frequency RSAEs with frequencies above the TAE frequency ($f \approx$ 330-450 kHz) were also excited. The destabilization of such high-frequency RSAEs was previously reported in reversed-shear plasmas in JT-60U heated with the negative-ion NBI system [37], indicating a similarity between the fast-ion populations generated by high-energy N-NBI systems and the three-ion ICRF scenario at JET.

As follows from Fig. 5(b), the destabilization of these modes in JET plasmas requires the presence of passing fast deuterium ions in the MeV-range with a pitch parameter $\lambda \approx$ 0.3-0.5. Yet traditionally used ICRF scenarios generate a population of fast ions with $\lambda \approx 0$. In contrast, the three-ion ICRF scheme generates a substantial population of passing fast ions with larger values of $\lambda$, thereby enabling resonant interaction of fast ions with high-frequency RSAEs. This novel finding sheds light on why these modes have not been extensively studied at JET in the past. Moreover, the RF-accelerated passing deuterium ions also play a significant role in driving a local fast-ion current and modifying the $q$-profile. The generation of a plasma with an inverted $q$-profile with a minimum $q_{min} \approx$ 0.80-0.85 at $R_{min} \approx$ 3.2 m was independently confirmed by MSE measurements, as shown in Fig. 5(c).

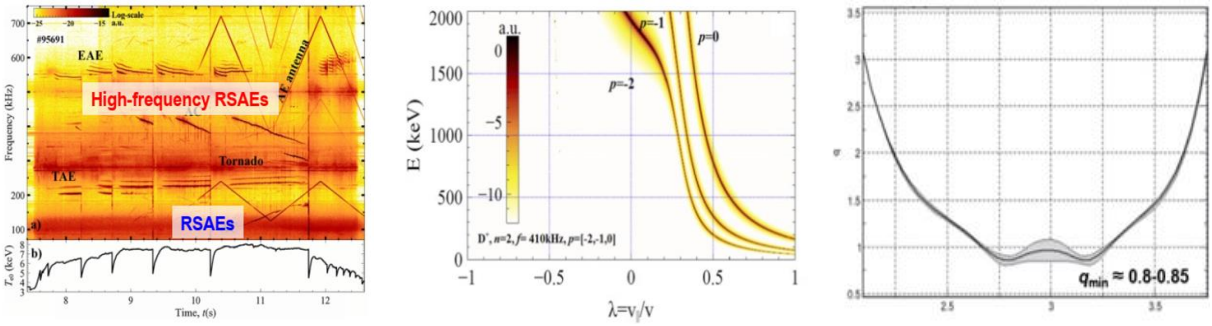


(a) (b) (c)

**FIGURE 5.** The three-ion D-($D_{NBI}$)-$^3$He ICRF scenario at JET was proven to be highly efficient for generating passing fast ions and for driving local current. This results in the formation of plasmas with an inverted $q$-profile and the destabilization of reversed-shear AEs, including high-frequency RSAEs, similar to earlier JT-60U observations with N-NBI heating [37]. (a) The high-frequency RSAEs with $f \approx$ 330-450 kHz ($n$ = 2) in JET pulse #95691. (b) The computed resonant map for the $n$ = 2 high-frequency RSAE interacting with D ions. (c) The $q$-profile in JET pulse #95691, as inferred by the MSE diagnostic. Reprinted with permission from M. Dreval et al., *Nucl. Fusion* **62**, 056001 (2022). Reproduced courtesy of IAEA. Copyright 2022 EURATOM.

These experiments also highlighted the impact of fusion-born alpha particles on the destabilization of different instabilities in the plasma. Indeed, the simultaneous observation of EAEs with the toroidal mode number $n = -1$ and the axisymmetric mode with $n = 0$ in the frequency range of EAEs was unexpected. According to the analysis in [35, 36], the destabilization of the $n = -1$ EAE requires the presence of high-energy ions with $\lambda < 0$, which are virtually absent in the fast-ion population generated by the three-ion ICRF scenario (see Fig. 4(a)). In contrast, the pitch-angle distribution of fusion-born alpha particles spans the entire range of pitch parameters from $\lambda = -1$ to $\lambda = +1$, therefore naturally providing a source of energetic ions with $\lambda < 0$. Furthermore, a new mechanism for sustaining bump-on-tail distributions of fusion-born alpha particles was identified. The sawtooth period in these experiments varied between 200-300 ms and a few seconds, and regular sawtooth crashes provided a natural modulation of the fusion power and the source of alphas. When the sawtooth period is shorter than the characteristic slowing-down time of the alpha particles, it can lead to the development of a bump-on-tail distribution for the alphas, thereby providing a source of free energy to destabilize the $n = 0$ mode [35, 36]. Recent studies in Ref. [38] investigated the energy-selective confinement of fusion-born alpha particles during sawtooth crashes in these JET plasmas.

The findings from these fast-ion experiments at JET and the emergence of new phenomena demonstrate the intricate and complex interplay between fast ions, monster sawtooth crashes, Alfvén eigenmodes, and plasma confinement. These surprising observations underscore the need for additional studies to thoroughly investigate the synergistic effects between different fast-ion phenomena in future burning plasmas, as also discussed in Ref. [25].

## PHYSICS STUDIES IN NON-ACTIVE H-$^4$HE PLASMAS ON AUG AND JET

Reaching good-quality H-mode and developing effective techniques for the control of edge-localized modes (ELMs) are among the main priorities for ITER during its non-active operations [39]. Recent promising experimental results at JET-ILW showed a significant reduction in the power threshold for H-mode transition in NBI-heated plasmas when a small amount of $^4$He ions, with a concentration of $n(^4\text{He})/n_e \approx 10\%$, was added to hydrogen plasmas [40]. This finding motivated the ITER team to consider the use of H-$^4$He plasmas to expand the H-mode operational space in predominantly hydrogen plasmas. Moreover, this plasma mixture also allows the application of the three-ion ICRF scheme with off-axis heating of $^3$He minority ions at concentrations of $n(^3\text{He})/n_e < 1\%$, as proposed in [41]. This enables the deposition of an additional 20 MW of heating power in H + 10% $^4$He plasmas in ITER.

The ASDEX Upgrade (AUG) tokamak was the first device to successfully demonstrate the integrated heating scenario with NBI, ECRF, and ICRF systems for its application in ITER [10]. Figure 6 shows an example of the application of the off-axis three-ion $^4$He-($^3$He)-H ICRF scenario on AUG (pulse #36751, 2.5T/0.8MA, $f \approx 30$MHz, dipole phasing). In this example, a ramp of ICRF power with off-axis $^3$He resonance was applied to trigger the L-H transition and ELMs (see Fig. 6(b)). Various combinations of heating systems were successfully applied to enter the H-mode on AUG, including NBI + ECRF + ICRF (as planned for ITER), ECRF + ICRF, and ICRF only. Studies at AUG also demonstrated that this off-axis ICRF scheme does not lead to tungsten accumulation.

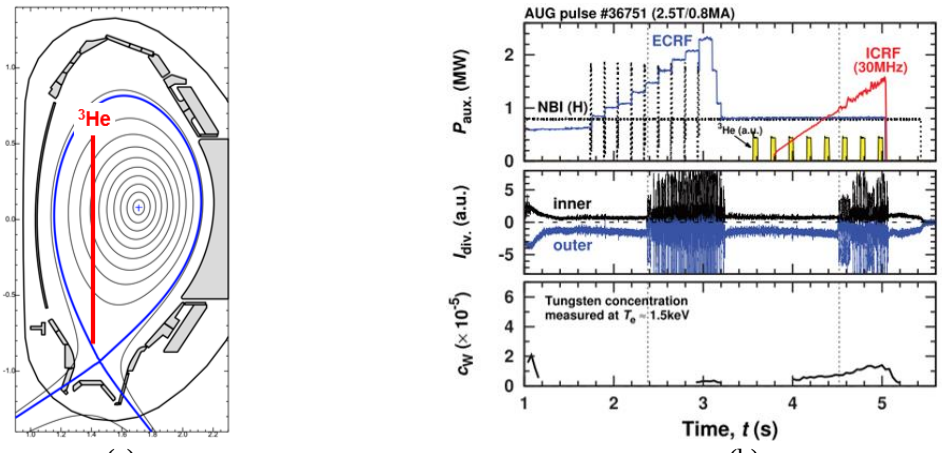


(a) (b)

**FIGURE 6.** The three-ion $^4$He-($^3$He)-H ICRF scenario with the off-axis $^3$He resonance is relevant for ITER operations. When combined with NBI and ECRF systems, this integrated heating scenario has the potential to expand the H-mode operational space in non-active ITER plasmas. (a) The magnetic configuration of AUG experiments with the off-axis $^3$He resonance in the plasma at 2.5T/0.8MA and $f \approx 30$ MHz. (b) The successful application of the three-ion $^4$He-($^3$He)-H ICRF scenario to trigger ELMs in H-$^4$He plasmas in AUG pulse #36751. The vertical dotted lines correspond to L-H transitions and the appearance of ELMs. Figure 6(b) reproduced with permission from Ye.O. Kazakov et al., *Phys. Plasmas* **28**, 020501 (2021). Copyright 2021 AIP Publishing.

The three-ion $^4$He-($^3$He)-H ICRF scheme with the off-axis $^3$He resonance was later successfully applied for plasma heating in H + ~10% $^4$He mixtures during the past hydrogen campaign at JET (2.5T/2.0MA, $f \approx 33$ MHz). However, the available auxiliary heating power in this campaign (no NBI, $P_{ICRF} \approx$ 3-4 MW) was not sufficient to trigger ELMs at this magnetic field and plasma conditions. As a result, JET focused on physics studies using the on-axis $^4$He-($^3$He)-H ICRF scheme at $B_0 = 3.2$T, as illustrated in Fig. 7. The high efficiency of this ICRF scenario for plasma heating was demonstrated utilizing an extremely small amount of $^3$He ions to absorb RF power, $n(^3\text{He})/n_e \approx 0.2\%$. Efficient plasma heating was achieved for a wide range of $^4$He concentrations, varying from ~5% to ~15%. The concentrations of both helium isotopes, $^4$He and $^3$He, were measured simultaneously using an improved sub-divertor gas spectroscopy [42].

Indeed, the very first pulse of these studies yielded successful results, as evidenced by an overview of JET pulse #98423 with the stepwise increase of ICRF power (3.2T/2.0MA, $n_{e0} \approx 4\times10^{19}$ m$^{-3}$, $f \approx 33$ MHz, dipole phasing), displayed in Fig. 7(b). According to TRANSP-TORIC modeling, more than 90% of the RF power was absorbed by a small fraction of $^3$He ions under these conditions, resulting in their acceleration to MeV-range energies. Subsequently, as a result of collisional slowing down, the ICRF-accelerated $^3$He ions deposited most of their energy to the plasma electrons ($E_{crit} \approx 41T_e \approx 160$ keV), leading to core-peaked electron heating, resembling the anticipated conditions for alpha heating in ITER and future fusion reactors.

The efficient generation of confined energetic $^3$He ions with ICRF was confirmed by various fast-ion diagnostics, including gamma-ray spectroscopy measurements. Additionally, the presence of fast $^3$He ions in the plasma resulted in the destabilization of different AEs and an increase in the neutron rate, as depicted in Fig. 7(b). In these non-active H-$^4$He plasmas, the neutrons originated from the fusion reactions between MeV-range ICRF-accelerated $^3$He ions and intrinsic $^9$Be impurities. Recently, an assessment of the impact of energetic ions on neutron yield during the pre-DT phase of ITER operations was reported in Ref. [43].

The efficiency of fast-ion generation was further improved by reducing the central plasma density to $n_{e0} \approx 3.5\times10^{19}$ m$^{-3}$ and increasing the RF power to 4MW, as shown in Fig. 7(c) (pulse #98433, solid lines). In this pulse, an asymmetric $+\pi/2$ ICRF antenna phasing was utilized, and a rich variety of Alfvén eigenmodes were observed, including reversed-shear AEs. This result confirms previous findings that three-ion ICRF scenarios can effectively modify the $q$-profile in the central regions of JET plasmas [10, 32]. For comparison, Fig. 7(c) also shows the response of the plasma under the same operational conditions but when the $-\pi/2$ ICRF antenna phasing was applied for plasma heating (pulse #98436, dotted lines). As expected from theory, the fast-ion generation efficiency was lower in pulse #98436, as evidenced by a much shorter sawtooth period $\Delta t_{saw} \approx 150$ ms as compared $\Delta t_{saw} \approx 470$ ms in pulse #98433.

The three-ion ICRF scheme with core $^3$He resonance was also applied in AUG (although in mixed H-D plasmas). However, due to the reduced confinement of MeV-range fast ions in AUG, setting up core plasma heating with this scenario is more challenging compared to a large-scale tokamak like JET, as discussed in Ref. [10]. Nonetheless, several novel fast ion measurements were developed with this scenario on AUG, including fast $^3$He measurements using charge exchange recombination spectroscopy [44] and $^3$He-driven ion cyclotron emission (ICE) [45]. These measurements provided valuable insights into the behavior and characteristics of fast He ions in tokamak plasmas.

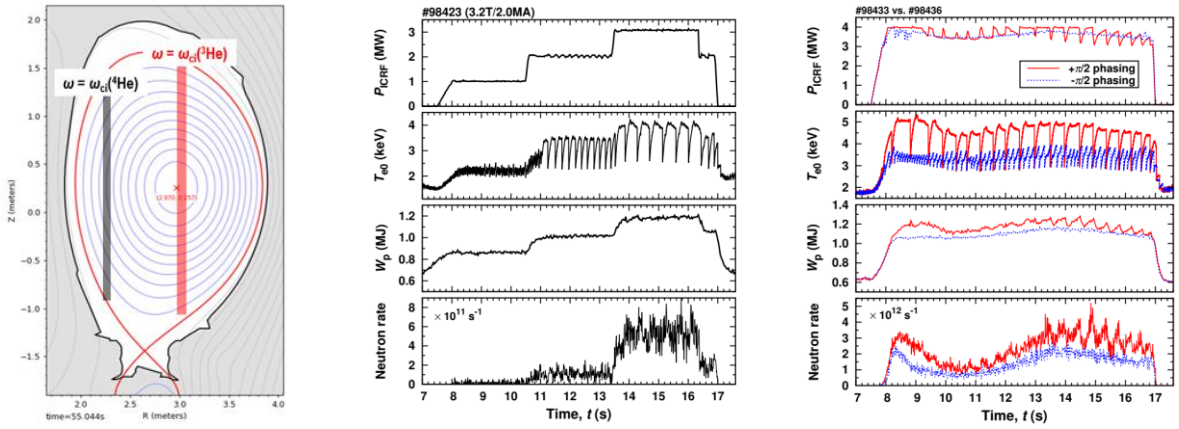


(a) (b) (c)

**FIGURE 7.** Demonstration of the successful application of the three-ion $^4$He-($^3$He)-H ICRF scenario with on-axis $^3$He resonance in non-active H-$^4$He plasmas at JET. The scheme proved to be efficient for a wide range of $^4$He concentrations, ranging from $n(^4\text{He})/n_e \approx 5\%$ to ~15%. (a) The magnetic configuration of JET experiments and the on-axis location of the $^3$He ion cyclotron resonance in the plasma at 3.2T/2.0MA, $f \approx 33$ MHz. (b) Overview of JET pulse #98423 with $n(^4\text{He})/n_e \approx 13\%$ and $n(^3\text{He})/n_e \approx 0.2\%$ (dipole phasing). (c) Overview of JET pulses #98433 ($+\pi/2$ phasing) and #98436 ($-\pi/2$ phasing) with $n(^4\text{He})/n_e \approx 8\%$ and $n(^3\text{He})/n_e \approx 0.2\%$, illustrating the impact of different antenna phasing on the efficiency of the fast-ion generation in the plasma.

# IMPURITY SEEDING AS A TOOL TO OPTIMIZE ICRF DEPOSITION AND GENERATION OF FAST $^4$HE IONS IN HYDROGEN PLASMAS

Impurity ions in multi-ion species plasmas can significantly contribute to the polarization and absorption of RF waves. A combination of intrinsic and extrinsic impurities can be applied as an active tool to control the deposition of ICRF power in fusion plasmas. In this section, we discuss the successful application of impurity seeding to enhance the efficiency of the generation of MeV-range $^4$He ions with ICRF in predominantly hydrogen plasmas at JET-ILW. Because $(Z/A)_{9Be} < (Z/A)_{4He} < (Z/A)_H$, intrinsic $^9$Be impurities ($Z = 4$, $A = 9$, and $Z/A \approx 0.44$) are not resonant absorbers in these plasmas, but are a crucial component that defines the efficiency of acceleration of resonant $^4$He ions ($n(^4\text{He})/n_e \approx 0.5\%$) with the three-ion $^9$Be-($^4$He)-H ICRF scenario.

According to theoretical and modeling results, $^4$He acceleration to high energies with this scenario is maximized at $^9$Be concentrations $n(^9\text{Be})/n_e \approx 1.5\text{-}2.5\%$ [46]. However, typical concentrations of $^9$Be impurities in JET-ILW plasmas are lower, $n(^9\text{Be})/n_e \approx 0.5\text{-}1.0\%$. As controlling the concentration of $^9$Be impurities in the plasma is not straightforward, injecting extrinsic impurities with a similar charge-to-mass ratio, such as $^7\text{Li}^{3+}$, $^{11}\text{B}^{5+}$, $^{22}\text{Ne}^{10+}$, $^{40}$Ar, etc., was proposed as an additional tool to optimize ICRF deposition [10, 46].

Figure 8 illustrates the first application of this novel technique in JET pulse #98503 (3.47T/2.0MA, $P_{ICRF} \approx 3$MW, $f \approx 29$ MHz, dipole phasing), which was conducted during the past hydrogen campaign at JET. Prior to this experiment, a series of ICRF experiments in H + ~10% $^4$He mixed plasmas was carried out (as reported in the previous section). As a result, even though no $^4$He gas was injected in pulse #98503, the residual level of $^4$He ions reached $n(^4\text{He})/n_e \approx 0.5\%$. Figure 8(a) illustrates the magnetic configuration in this JET pulse, together with the location of the ion cyclotron resonance for resonant $^4$He ions, as well as for non-resonant H ions and $^9$Be impurities. Under the selected experimental conditions, the cyclotron resonance of resonant $^4$He ions was located ~30 cm off-axis. However, locating the cyclotron resonance of $^4$He ions in the plasma core would require a significantly higher magnetic field strength of around 3.85T. Unfortunately, due to limitations at such high magnetic field strengths at JET, plasma operation with this magnetic configuration could not be realized during the time of the experiment.

Figure 8(b) shows an overview of the main parameters in JET pulse #98503, including the plasma stored energy, the central electron temperature, and the neutron rate. Note that these parameters were increased during the last phase of the pulse when a small amount of $^{22}$Ne impurities ($Z = 10$, $A = 22$, and $Z/A \approx 0.45$) with a charge-to-mass ratio similar to $^9$Be impurities, were injected into the plasma. Moreover, during the phase with $^{22}$Ne injection, a more efficient sawtooth stabilization was observed. Additionally, gamma-ray diagnostics confirmed the efficient generation of MeV-range $^4$He ions with the three-ion $^9$Be/$^{22}$Ne-($^4$He)-H ICRF scenario. This novel ICRF scenario was developed and applied to prepare and validate alpha particle diagnostics for their future use in the D-T campaign, complementing earlier developments with the three-ion D-($D_{NBI}$)-$^3$He scheme [27].

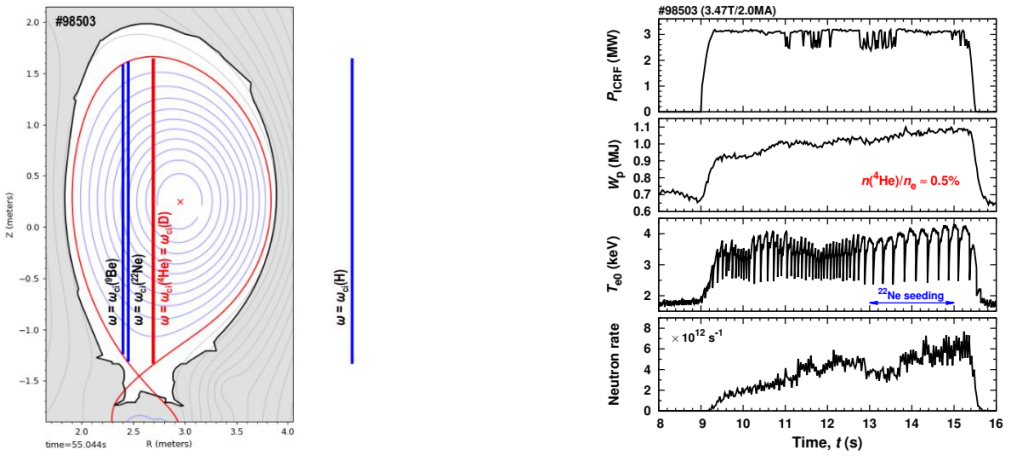


(a) (b)

**FIGURE 8.** The proof-of-principle demonstration of the three-ion $^9$Be/$^{22}$Ne-($^4$He)-H ICRF scenario for plasma heating and generation of MeV-range $^4$He ions in H majority plasmas was carried out at JET-ILW [10, 46]. (a) The magnetic configuration and the location of the ion cyclotron resonances for H, $^4$He (resonant ions), $^9$Be, and $^{22}$Ne species in JET pulse #98503 (3.47T/2.0MA, $f \approx 29$ MHz, dipole phasing). (b) Overview of the main parameters in JET pulse #98503 ($n(^4\text{He})/n_e \approx 0.5\%$). A more efficient generation of MeV-range $^4$He ions was achieved during the last phase of the pulse, when an additional seeding of $^{22}$Ne impurities was applied.

# USING IMPURITIES FOR BULK ION HEATING OF D-T ≈ 50%-50% PLASMAS

During recent tritium and DTE2 campaigns at JET-ILW, several ICRF scenarios were successfully developed and applied for heating tritium, T-rich and D-T ≈ 50%-50% plasmas [47-50]. In ITER, second harmonic ICRF heating of fuel tritium ions, $\omega = 2\omega_{ci}$(T) is considered as the main ICRF heating scenario in D-T ≈ 50%-50% plasmas [2, 51]. In order to increase the fraction of bulk ion heating, this heating scenario also foresees injecting a few percent of $^3$He ions to absorb RF power during the ramp-up phase of the pulse. However, as $^3$He is a scarce gas, an alternative scenario using intrinsic $^9$Be impurities as resonant absorbers for increasing the ion temperature in D-T ≈ 50%-50% plasmas was proposed [52]. One of the advantages of using $^9$Be impurities is their significantly larger critical energy compared to $^3$He ions (with $E_{crit}(^9\text{Be}) \approx 74T_e$ vs. $E_{crit}(^3\text{He}) \approx 25T_e$). This allows $^9$Be impurities to transfer a larger fraction of absorbed RF power to the fuel D and T ions through Coulomb collisions.

During the recent DTE2 campaign at JET, the novel three-ion T-($^9$Be)-D ICRF scenario with intrinsic $^9$Be impurities ($n(^9\text{Be})/n_e \approx 0.5$-1.0%) was successfully demonstrated for increasing the plasma stored energy and the ion temperature, as shown in Fig. 9(a). In pulse #99608 (3.7T/2.0MA, L-mode, D-T ≈ 50%-50%, $n_{e0} \approx 4\times10^{19}$ m$^{-3}$) with $P_{NBI} \approx$ 4-6 MW (tritium, $E_{NBI} \approx$ 100-110 keV) and $P_{ICRF} \approx 2$ MW ($f \approx$ 25MHz, dipole phasing), the ion cyclotron resonance of $^9$Be impurities was located in the plasma core during the flat-top phase of the pulse. The heating performance of ICRF (defined as the increase of the plasma stored energy per MW of auxiliary heating power) reached $\Delta W_p/\Delta P_{ICRF} \approx 0.30$ MJ/MW, significantly larger than the corresponding value for the NBI system in this pulse ($\Delta W_p/\Delta P_{NBI} \approx 0.20$ MJ/MW). In line with theoretical predictions, a strong increase in $T_i$ was observed when ICRF power was coupled to the plasma, see the red dotted line in the second panel of Fig. 9(a). Neutron and gamma-ray diagnostics confirmed the generation of fusion-born alpha particles localized in the plasma core. After the switch off NBI system at $t = 11.0$ s, the toroidal magnetic field was ramped down, reaching $B_t \approx 3.46$T at $t = 12.4$ s. Figure 9(a) also illustrates that efficient plasma and $T_i$ heating were achieved during this ICRF-only phase, when the location of the ion cyclotron resonance layer of $^9$Be impurities was gradually shifted from the plasma core ($R \approx 3.0$ m) to the HFS off-axis ($R \approx 2.8$ m).

The three-ion T-($^9$Be)-D ICRF scheme was also successfully demonstrated for heating H-mode D-T plasmas in JET pulse #99982 (3.7T/2.5MA), which was the last pulse of the DTE2 campaign. Figure 9(b) demonstrates that >8 MW of fusion power was sustained for 2.5 s with a combination of high-power NBI (deuterium, $P_{NBI} \approx 29$ MW) and ICRF heating tuned to the core cyclotron resonance of $^9$Be impurities ($P_{ICRF} \approx 1.7$MW, $f \approx$ 25MHz, dipole phasing). In pulse #99982, the maximum fusion power $P_{fus} \approx 9$ MW ($R_\alpha \approx 3.1\times10^{18}$ s$^{-1}$) was achieved at $t \approx$ 9.5-9.6 s, when the isotopic ratio reached D-T ≈ 40%-60%. Under these experimental conditions, the RF power is partly absorbed by $^9$Be impurities, deuterons and alphas [10, 53]. Modeling of the exact split of the absorbed RF power between the different ion populations is not straightforward and the results will be reported elsewhere.

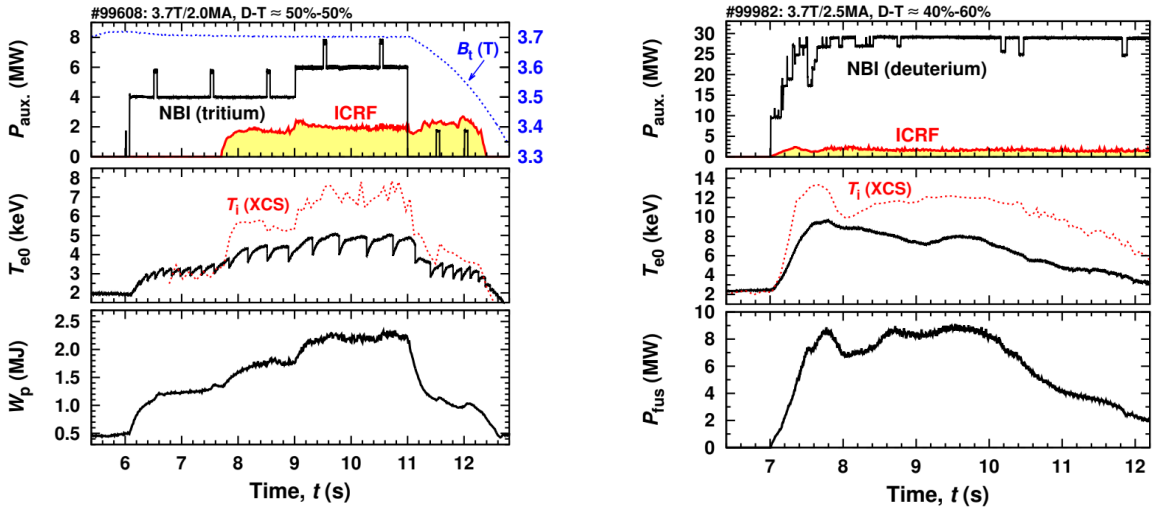


(a) (b)

**FIGURE 9.** The successful demonstration of the ITER-relevant three-ion T-($^9$Be)-D ICRF scenario for plasma heating and increasing ion temperature in D-T plasmas at JET-ILW. (a) Overview of JET pulse #99608 (L-mode, 3.7T/2.0MA, D-T ≈ 50%-50%); (b) Overview of JET pulse #99982 (H-mode, 3.7T/2.5MA, D-T ≈ 40%-60%). In both pulses, ICRF settings ($f \approx$ 25 MHz, dipole phasing) were selected to position the cyclotron resonance of $^9$Be impurities in the plasma core.

As discussed in Refs. [10, 52], the three-ion T-($^{9}$Be)-D ICRF scenario is compatible with additional seeding of impurities such as $^{7}$Li, $^{11}$B, $^{22}$Ne, and Ar. This expands the potential application of this scenario in ITER and future fusion reactors. Although the experimental study of combined Ar and $^{9}$Be ICRF heating of D-T plasmas was planned as a part of DTE2 studies, it was not conducted due to limited machine time.

Finally, we note that off-axis plasma heating using a similar T-($^{7}$Li)-D ICRF scenario was previously observed in earlier D-T experiments on TFTR, but was considered as a negative result, attributed to parasitic RF absorption by $^{7}$Li impurities [54]. However, recent studies have re-evaluated the potential of this ICRF scenario, and the three-ion T-($^{7}$Li)-D ICRF scenario has been proposed for bulk ion heating in CFETR [55].

## SUMMARY AND CONCLUSIONS

Significant advancements with the development of three-ion ICRF scenarios on the tokamaks Alcator C-Mod, ASDEX Upgrade and JET have opened up new possibilities for plasma heating and fast-ion studies in fusion plasmas [8, 10]. When tuned for depositing RF power in the plasma core and maximizing fast-ion pressure, these scenarios have provided a better understanding of plasmas with core electron heating from fast ions in the MeV-range. Analysis of dedicated JET experiments in D-$^{3}$He plasmas has revealed a range of new physics phenomena relevant to ITER and future fusion reactors with dominant alpha particle heating. Improved thermal ion confinement was observed in JET plasmas with a large amount of MeV-range fast ions, despite the destabilization of a large variety of Alfvén eigenmodes [29]. JET experiments also demonstrated the potential of these ICRF scenarios for generating a large population of passing fast ions, which can be applied for local current drive and sustaining plasmas with an inverted $q$-profile in the plasma core [10, 32].

Three-ion ICRF scenarios are also relevant for plasma operations in ITER. Recent progress in non-active and D-T plasmas at JET and ASDEX Upgrade has shown promising results. For example, ASDEX Upgrade has prototyped the integrated scenario with NBI, ECRF and ICRF systems for heating H-$^{4}$He plasmas, which has the potential to expand the H-mode operational space in ITER [10, 41].

Furthermore, recent JET experiments in non-active and D-T plasmas have shown that these novel ICRF scenarios can benefit from the presence of low-$Z$ and mid-$Z$ impurities in the plasma. For instance, the improved efficiency of the generation of MeV-range $^{4}$He ions with ICRF was demonstrated at JET, when Be-like impurities, such as $^{22}$Ne, were injected into the hydrogen majority plasma. Moreover, dedicated JET-ILW experiments with the three-ion T-($^{9}$Be)-D scenario in D-T plasmas have demonstrated that the intrinsic level of $^{9}$Be impurities ($n(^{9}\mathrm{Be})/n_{e} \approx 0.5$-$1.0\%$) is sufficient to achieve the high efficiency of bulk ion heating and increasing the ion temperature in D-T $\approx$ 50%-50% plasmas, which is also relevant for ITER [52].

## ACKNOWLEDGMENTS

This work has been carried out within the framework of the EUROfusion Consortium, funded by the European Union via the Euratom Research and Training Programme (Grant Agreement No 101052200 – EUROfusion). Views and opinions expressed are however those of the author(s) only and do not necessarily reflect those of the European Union or the European Commission. Neither the European Union nor the European Commission can be held responsible for them. We thank the ITPA Energetic Particle Physics Topical Group for its support. Part of this work was also carried out in the framework of projects done for the ITER Scientist Fellow Network (ISFN).

ITER is the Nuclear Facility INB No. 174. The views and opinions expressed herein do not necessarily reflect those of the ITER Organization. This publication is provided for scientific purposes only. Its contents should not be considered as commitments from the ITER Organization as a nuclear operator in the frame of the licensing process.

See the author list of J. Mailloux et al., *Nucl. Fusion* **62**, 042026 (2022) for the list of JET Contributors; see the author list of H. Meyer et al., *Nucl. Fusion* **59**, 112014 (2019) for the ASDEX Upgrade Team; see the author list of B. Labit et al., *Nucl. Fusion* **59**, 086020 (2019) for the EUROfusion MST1 Team.

## REFERENCES

1. M. Porkolab et al., AIP Conf. Proc. **314**, 99 (1994)
2. ITER Physics Basis Expert Group on Energetic Particles, Heating and Current Drive and ITER Physics Basis Editors, Nucl. Fusion **39**, 2495 (1999)
3. J. Ongena et al., Plasma Phys. Control. Fusion **59**, 054002 (2017)
4. J.R. Wilson and P.T. Bonoli, Phys. Plasmas **22**, 021801 (2015)

5. T.H. Stix, Nucl. Fusion **15**, 737 (1975)
6. T.H. Stix, Plasma Phys. **14**, 367 (1972)
7. Ye.O. Kazakov et al., Nucl. Fusion **55**, 032001 (2015)
8. Ye.O. Kazakov et al., Nature Physics **13**, 973 (2017)
9. J. Ongena et al., EPJ Web Conf. **157**, 02006 (2017)
10. Ye.O. Kazakov et al., Phys. Plasmas **28**, 020501 (2021)
11. D. Van Eester et al., Plasma Phys. Control. Fusion **54**, 074009 (2012)
12. Ye.O. Kazakov et al., Plasma Phys. Control. Fusion **52**, 115006 (2010)
13. Y. Lin et al., EPJ Web Conf. **157**, 03030 (2017)
14. D. Van Eester et al., Plasma Phys. Control. Fusion **59**, 085012 (2017)
15. Ye.O. Kazakov et al., AIP Conf. Proc. **1689**, 030008 (2015)
16. L.-G. Eriksson et al., Phys. Rev. Lett. **81**, 1231 (1998)
17. M.J. Mantsinen et al., Phys. Rev. Lett. **89**, 115004 (2002)
18. H. Järleblad et al., Nucl. Fusion **62**, 112005 (2022)
19. Ye.O. Kazakov et al., Nucl. Fusion **60**, 112013 (2020)
20. K. Kirov et al., AIP Conf. Proc. **2254**, 030011 (2020)
21. M.J. Mantsinen et al., Proc. 46th EPS Conf. on Plasma Physics, O5.102 (2019)
22. A. Sahlberg et al., Nucl. Fusion **61**, 036025 (2021)
23. V. Bobkov et al., AIP Conf. Proc. **2254**, 040005 (2020)
24. J. Garcia et al., Phys. Plasmas **25**, 055902 (2018)
25. S. Pinches et al., Phys. Plasmas **22**, 021807 (2015)
26. M. Nocente et al., Nucl. Fusion **60**, 124006 (2020)
27. E. Panotin et al., Rev. Sci. Instrum. **92**, 053529 (2021)
28. J. Mailloux et al., Nucl. Fusion **62**, 042026 (2022)
29. S. Mazzi et al., Nature Physics **18**, 776 (2022)
30. S. Mazzi et al., Plasma Phys. Control. Fusion **64**, 114001 (2022)
31. Ž. Štancar et al., Nucl. Fusion **61**, 126030 (2021)
32. M. Dreval et al., Nucl. Fusion **62**, 056001 (2022)
33. A. Tinguely et al., Nucl. Fusion **62**, 076001 (2022)
34. A. Tinguely et al., Nucl. Fusion **62**, 112008 (2022)
35. V.G. Kiptily et al., Nucl. Fusion **61**, 114006 (2021)
36. V.G. Kiptily et al., Plasma Phys. Control. Fusion **64**, 064001 (2022)
37. M. Takechi et al., Phys. Plasmas **12**, 082509 (2005)
38. A. Bierwage et al., Nature Comm. **13**, 3941 (2022)
39. B. Bigot, Nucl. Fusion **59**, 112001 (2019)
40. J.C. Hillesheim et al., Proc. 44th EPS Conf. on Plasma Physics, P5.162 (2017)
41. M. Schneider et al., EPJ Web Conf. **157**, 03046 (2017)
42. S. Vartanian et al., Fusion Eng. Design **170**, 112511 (2021)
43. A. Polevoi et al., Nucl. Fusion **61**, 076008 (2021)
44. A. Kappatou et al., Nucl. Fusion **61**, 036017 (2021)
45. R. Ochoukov et al., AIP Conf. Proc. **2254**, 030005 (2020)
46. Ye.O. Kazakov et al., Proc. 45th EPS Conf. on Plasma Physics, P5.1047 (2018)
47. P. Jacquet et al., "ICRH operations and experiments during the JET-ILW tritium and DTE2 campaign", this conference
48. K. Kirov et al., "Impact of ICRH heating of fast D and T ions on fusion performance in JET DTE2 campaign", this conference
49. E. Lerche et al., "Fundamental ICRF heating of Deuterium ions in JET-DTE2", this conference
50. D. Van Eester et al., "RF power as key contributor to high performance baseline scenario experiments in JET DD and DT plasmas in preparation for ITER", this conference
51. M. Mantsinen et al., "Experiments in high-performance JET plasmas in preparation of second harmonic ICRF heating of tritium in ITER", Nucl. Fusion (submitted)
52. Ye.O. Kazakov et al., Phys. Plasmas **22**, 082511 (2015)
53. E. Lerche et al., AIP Conf. Proc. **2254**, 030007 (2020)
54. J.R. Wilson et al., Phys. Plasmas **5**, 1721 (1998)
55. C. Song et al., Physica Scripta **96**, 025603 (2021)